

Fragility Curves for Limited Ductile Reinforced Concrete Buildings

E. Lumantarna^{1,4}, N. Lam^{1,4}, H.H. Tsang^{2,4}, J. Wilson^{3,4}, E. Gad^{2,4} and H. Goldsworthy^{1,4}

¹ Department of Infrastructure Engineering, The University of Melbourne, Parkville, Victoria, Australia

² Faculty of Science, Engineering and Technology, Swinburne University of Technology, Melbourne, Victoria, Australia

³ Swinburne University of Technology, Sarawak Campus, Kuching, Sarawak, Malaysia

⁴ Bushfire and Natural Hazards Cooperative Research Centre (BNHCRC)

ABSTRACT

Reinforced concrete buildings make up the majority of Australian building stocks. Structural elements of these buildings are often designed with limited to nonductile detailing. With a very low building replacement rate many of the Australian buildings are vulnerable to major earthquakes and pose significant risk to lives, properties and economic activities.

This paper presents studies on seismic vulnerability assessments of limited ductile reinforced concrete buildings. Fragility curves have been developed for three types of buildings, buildings that are mainly supported by shear or core walls, buildings that are supported by shear walls and moment resisting frames and podium-tower buildings featuring a transfer structure. The studies form a part of a collaborative research under the Bushfire and Natural Hazards Cooperative Research Centre (BNHCRC) on “cost-effective mitigation strategy development for building related earthquake risk”.

Keywords: fragility curves, limited ductile reinforced concrete, seismic vulnerability assessment

1 Introduction

The project “Cost-Effective Mitigation Strategy Development for Building Related Earthquake Risk” under the Bushfire and Natural Hazards Cooperative Research Centre (BNHCRC) aims to develop knowledge to facilitate evidence-based informed decision making in relation to the need for seismic retrofitting, revision of codified design requirement, and insurance policy.

Cost-benefit analysis will be used as a standard tool to facilitate informed decision making. Apart from developing socio-economic loss models which are relevant to costing, seismic vulnerability assessment of different forms of structures is an essential component of the project. The current platform used in Australia for earthquake loss estimation is the Earthquake Risk Model (EQRM) (Robinson et al., 2005), which adopts the methodology used by HASUS (FEMA, 2010). However, buildings in Australia are usually designed with little to no consideration for ductile detailing and are generally more vulnerable than buildings in more seismically active regions (Edwards et al., 2004).

This paper presents a summary of the studies conducted by the project team in conjunction with PhD students who are financially supported by the BNHCRC project. Sets of fragility curves which are essential inputs to cost-benefit analysis are presented for limited-ductile reinforced concrete (RC) buildings typical of Australian constructions: i) fragility curves for RC buildings that are primarily supported by limited-ductile RC shear walls (referred to **RC shear walls buildings** herein); ii) fragility curves for RC buildings that are supported by limited-ductile RC walls and frames (referred to **RC frames buildings** herein); and iii) fragility curves for **podium-tower RC buildings**. For full details, the readers are referred to Amirsardari (2018), Hoult et al. (2018a) and Yacoubian (2018). The details of the buildings are presented in Section 2 and the modelling of the buildings for non-linear analyses are presented in Section 3. The selection of ground motion inputs for the analyses is presented in Section 4. The development of the fragility curves is presented in Section 5.

2 Description of buildings

The following sections present the configuration of buildings and design of structural elements adopted in this study.

2.1 RC shear walls buildings

Four idealised reinforced concrete shear walls buildings, laterally supported by rectangular and/or RC walls, were used in the assessment. The four configurations considered are presented in Figure 1. The height of the buildings varies from 2-storey to 12-storey high. The type of RC shear wall configuration was selected for each building depending on the capability of the walls in resisting earthquake and wind load in accordance with Australian Standard (AS1170.4-2007; AS1170.2:2011).

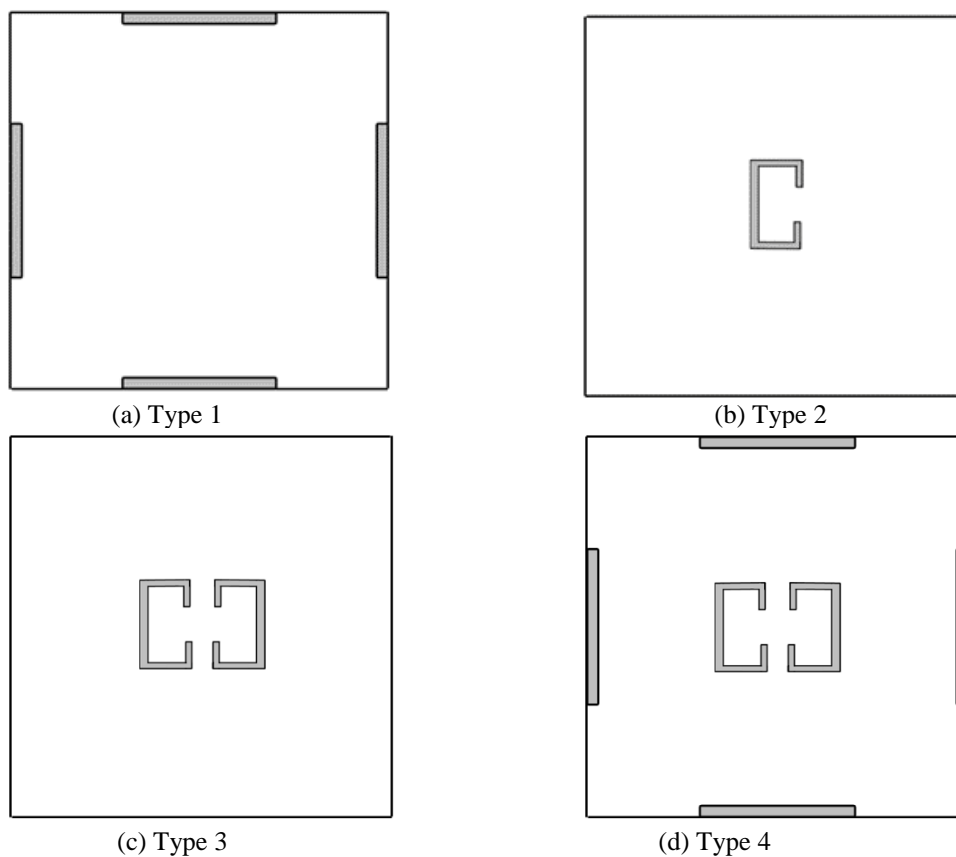


Figure 1 Idealised RC shear walls buildings

Table 1 presents the building types (according to the wall configuration) and the associated minimum and maximum number of storeys that can be supported by each building type. The definition of the low-rise, mid-rise and high-rise corresponds to the number of storeys has been adopted from (FEMA, 2010). This definition has also been adopted in Geoscience Australia's Earthquake Risk Model (EQRM) (Robinson, 2005).

The building parameters such as the axial load ratio (ALR), dead (G) and live (Q) load, inter-storey height (h_s) and longitudinal reinforcement ratio (ρ_{wv}) were varied between the maximum and minimum values summarised in Table 2. The length of the rectangular walls (L_w) was selected randomly between a value of $0.17B$ and $0.33B$, where the width of the building (B). The dimensions of the C-shaped walls for Building Types 2, 3 and 4 in Figure 1 were based on the number of storeys and are presented in Table 3.

Table 1 Building Types with limiting number of storeys (n)

Building Type	minimum n	maximum n	Rise
1	2	4	Low, Mid
2	2	3	Low
3	2	7	Low, Mid
4	4	12	Mid, High

Table 2 Wall parameters and values considered for the assessment

Parameter	μ	σ	min	max	Constant	Units
ALR	-	-	0.01	$0.1^a/0.05^b$	-	-
G	-	-	4	8	-	kPa
Q	-	-	1	4	-	kPa
h_s	-	-	3.0	3.5	-	M
ρ_{wv}	-	-	0.19%	1.00%	-	-

^a = Rectangular walls

^b = C-shaped Walls

Table 3 Dimensions of the C-shaped walls

Wall	t_w (mm)	L_{web} (mm)	L_{flange} (mm)	L_{return} (mm)
Low-rise	200	3600	2000	600
Medium-rise	200	6200	2200	600
High-rise	250	8500	2500	600

2.2 RC frames buildings

Three reinforced concrete buildings were assessed which are 2-storey, 5-storey and 9-storey high, representing low-, medium- and high-rise buildings. The buildings are representative of older RC buildings constructed in Australia prior to the requirement for seismic load and design to be mandated on a national basis. The buildings have been designed in accordance with AS 3600:1988 Concrete Structures Standard, AS 1170.2:1983 Wind Actions Standard, and guidance from experienced practicing structural engineers. The frames were designed as ordinary moment resisting frames (OMRFs). The core walls have low longitudinal reinforcement ratio (approximately 0.23 %) with no confinement. The building plans are provided in Figure 2. The gravity load resisting system of the buildings constructed in the 1980s typically included perimeter frames with deep beams (600-900 mm deep) to satisfy fire design

requirements, and band-beams or flat-slab floor systems with column spacing of 7.0 to 8.4 m. Hence for the buildings the typical column spacing of 8.4 m was adopted with perimeter beam depth of 650 mm. The design properties of the building components are presented in Table 4.

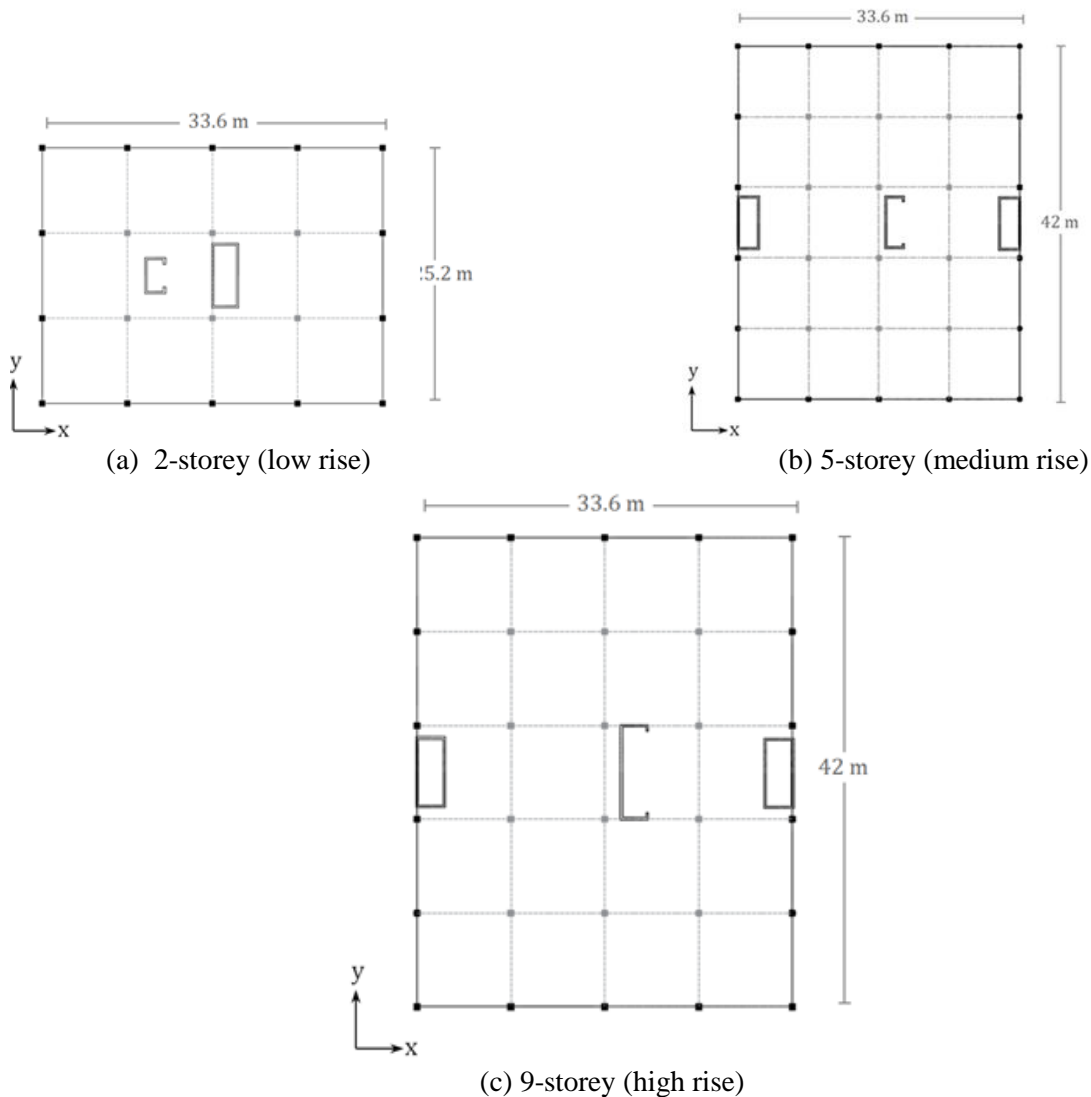


Figure 2 Idealised RC frames buildings

Table 4 Summary of design properties for building components

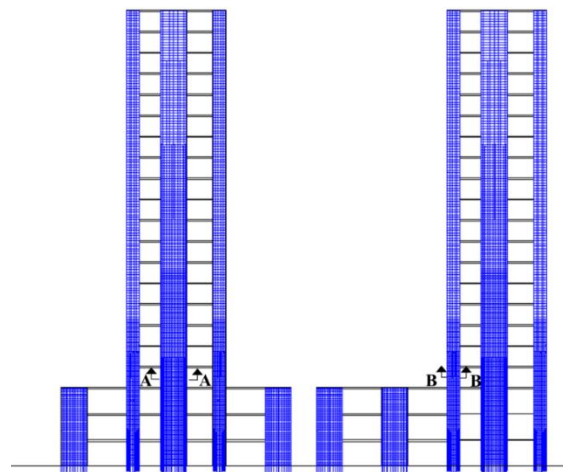
	Slab	Perimeter beams	Columns	Core walls
f'_c (MPa)	25	25	40	40
f_y (MPa)	400	400	400	400
ρ_l (%)	0.67-1.33	1.30-2.70	2.0-4.0	0.23-0.24
ρ_t (%)	0.25	0.23	0.075-0.12	0.25

f'_c : characteristic concrete compressive strength | f_y : nominal reinforcement yield strength | ρ_l : longitudinal reinforcement ratio | ρ_t : transverse reinforcement ratio

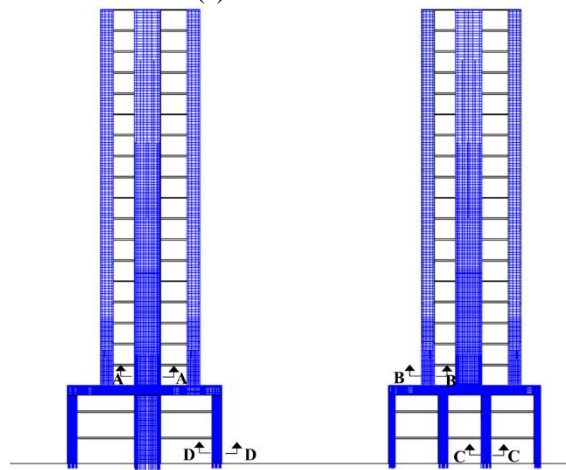
2.3 Podium-tower RC buildings

Two groups of podium-tower RC buildings were assessed. The first group consists of two buildings featuring a setback in the floor plan above the podium level (SB-1 and SB-2). The second group consists of two buildings featuring a transfer plate. The tower structure of all the

building models comprises of three walls connected by floor slabs. The elevation views of the buildings are shown in Figure 3. In the first group (setback buildings), the tower structure is continued to the podium levels. Building model SB-1 has a tower structure that is centred on the supporting podium. Building model SB-2 has the tower structure at an offset from the centre of the building. For the second group (transfer structure), some or all of the structural elements at the tower structure are discontinued at the transfer floor level. Building model TS-1 has a continuous central wall which forms the primary lateral load resisting elements whilst the other walls are discontinued at the transfer floor level. In building TS-2, all three tower walls are discontinued at the transfer floor level. The podium structure of TS-2 consists of the stiff columns that are also coupled by floor slabs. Summary of the design properties of the building component are presented in Figure 4.

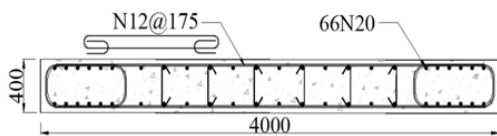


(a) SB-1 and SB-2



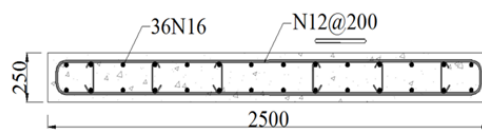
(b) TS-1 and TS-2

Figure 3 Elevation views of the podium-tower RC buildings



$\rho_l = 1.3\%$, $\rho_t = 0.32\%$
ALR = 0.12

RC walls Section A-A



$\rho_l = 1.15\%$, $\rho_t = 0.31\%$
ALR = 0.12

RC walls Section B-B

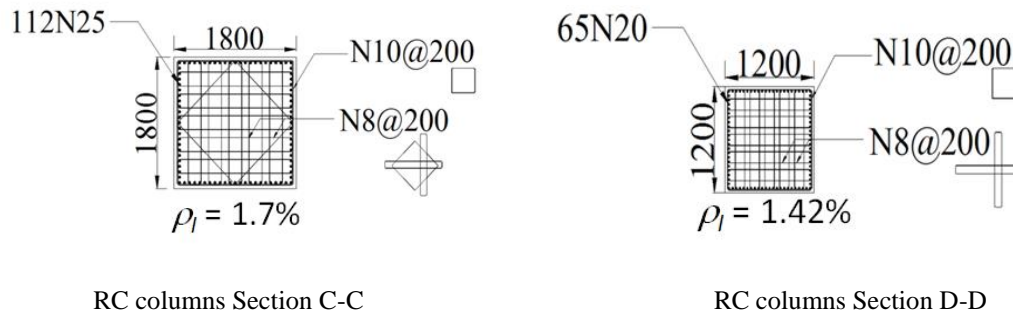


Figure 4 Details of typical structural elements

3 Modelling for non-linear analyses

The following sections present the modelling and analysis approach adopted to construct fragility curves of the limited ductile reinforced concrete buildings.

3.1 RC shear walls buildings

A large number of analyses for the RC shear walls buildings were undertaken using the capacity spectrum method. The method involves comparing the capacity curve of a structure to the seismic demand in the format of an acceleration-displacement response spectrum (ADRS) as illustrated schematically in Figure 5. The performance point (or “demand point” in Figure 5) is the location at which the two curves (with the same effective damping) intersect. This point provides an estimation of both the inelastic acceleration and displacement demand of a structure with a given earthquake.

The capacity curve of the walls for each building was constructed using moment-curvature analyses, based on the stress-strain (σ - ϵ) relationships given in Popovics (1973) and Seckin (1981), for concrete (normal and high strength concrete) and steel reinforcement, respectively. The moment-curvature analyses were used to obtain the ultimate moment, as well as curvature and moment values at different levels of strains associated with different performance levels. Based on the moment-curvature values at different performance levels, plastic hinge analyses were conducted to obtain the force displacement capacities of the walls. The calculations to determine the yield displacement (Δ_y) and plastic displacement (Δ_p) were based on the plastic hinge length (L_p) expressions derived by Hout et al. (2018b; 2018c; 2017).

The demand curve was constructed from individual earthquake ground motions in the acceleration and displacement demand format. The displacement capacity was used to modify the elastic acceleration and displacement demand spectra by the expressions of equivalent damping and spectral reduction factor from Priestley et al. (2007).

3.2 RC frames buildings

The assessment for RC frames buildings was performed using nonlinear dynamic time history analysis (NDTHA). The nonlinear models for the buildings presented in Figure 2 were created in the finite element analysis package OpenSEES (McKenna et al., 2000).

The concrete fibres were modelled using the Popovics (1973) uniaxial concrete stress-strain material model which is available in OpenSees as *Concrete04* and the reinforcement bars were modelled using the Giuffr -Menegotto-Pinto uniaxial material model (Menegotto & Pinto, 1973) which is available as *Steel02* model in OpenSEES. The material properties are based on the reported values from the experiments and are presented in Table 5.

Table 5 Input parameters adopted for Concrete04 material model

Input parameter	Unconfined concrete	Confined concrete
Concrete compressive strength	f_c	Confined concrete compressive strength: $f_{cc} = Kf_c$ where K is the confinement factor according to Mander et al., (1988)
Strain at maximum strength	$\varepsilon_{c0} = 0.002$	$\varepsilon_{cc0} = \varepsilon_{c0}(1 + 5(K - 1))$ (Mander et al, 1988)
Strain at crushing strain	$\varepsilon_{cu} = 0.012 - 0.0001f_c$ (Reddiar, 2009)	$\varepsilon_{ccu} = 5\varepsilon_{cc0} + 0.004$ (Reddiar, 2009)
Initial stiffness	$E = 5000\sqrt{f_c}$	$E = 5000\sqrt{f_c}$
Maximum tensile strength	$f_{ct} = 0.6\sqrt{f_c}$ (AS 3600: 2009)	$f_{ct} = 0.6\sqrt{f_c}$ (AS 3600: 2009)
Ultimate tensile strain	$\varepsilon_t = 0.1\varepsilon_{cu}$	$\varepsilon_t = 0.1\varepsilon_{cu}$

The columns, beams, and walls were modelled using lumped plasticity elements and the beam-column joint response was modelled using the scissor’s model with rigid links approach. The walls and the columns were assumed to be fixed to the ground. Furthermore, a rigid diaphragm was also assumed. *Pinching4* material model has been adopted to define the hysteretic behaviour of the structural elements. The values of the parameters defining the model were determined by calibration to experimental results published in the literature. Full details of the hysteretic modelling of the structural elements and the calibration can be found in Amirsardari (2018)

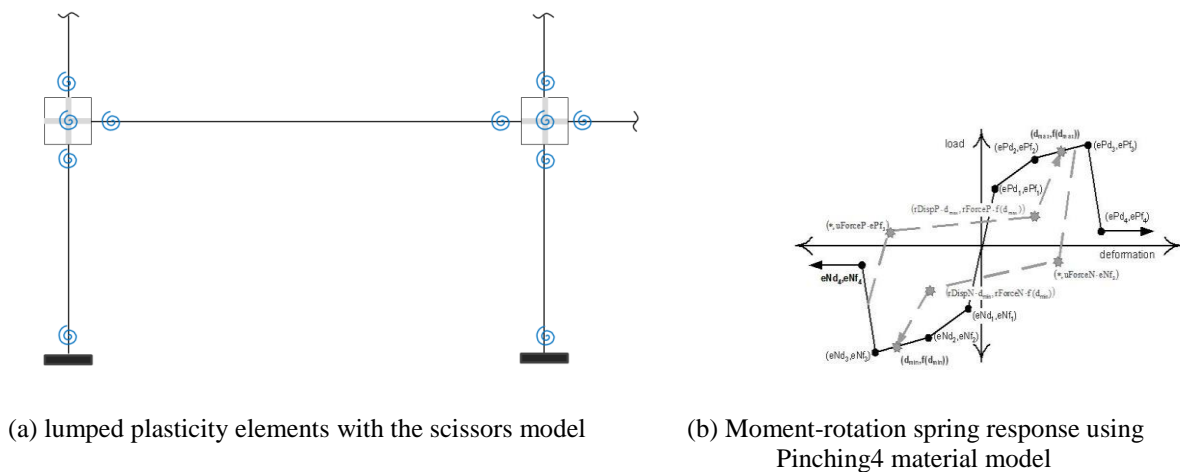


Figure 5 Non-linear modelling of beam and columns (Amirsardari, 2018)

3.3 Podium-tower RC buildings

The assessment of podium-tower RC buildings was conducted using NDTA. The inelastic numerical models of the buildings have been constructed on the SeismoStruct program (SeismoSoft, 2016). The distributed plasticity modelling approach using fibre-based inelastic frame element has been adopted in the modelling of the flexural response of the walls and the floors slabs. The fibre-based approach is able to preserve the axial-flexural interaction in the response behaviour of the members, which were particularly important for the modelling of the floor slabs and tower walls.

The reinforced concrete walls have been modelled with a combination of inelastic fibre-based elements and zero-length lumped shear springs that are connected in series as shown

schematically in Figure 6. The inelastic frame elements have been discretised at the sectional level (into various fibres) and at the elemental level. The tri-linear model recommended in ASCE41-13 (2013) and FEMA 356 (2000), which consists of three main phases, uncracked, post-cracked and post-peak behaviour, as shown schematically in Figure 6. The hysteretic behaviour of the shear sub-element (with tri-linear shear backbone) has been defined by the model developed by Sivalsevan and Reinhorn (2000). The pinching effect, which commonly characterises the shear response behaviour of shear-critical walls, was modelled by the slip parameter of 0.3 based on recommendations by Mergos and Beyer (2014). The Mander concrete constitutive model (Mander et al., 1988) has been adopted for modelling the uni-axial response behaviour of confined and unconfined concrete (fibres) whereas the modified Menegotto-Pinto (1973) constitutive relationship is adopted for the reinforcing steel. Expected material strength values were used instead of the design lower characteristic strength for both the concrete and steel. The values of the expected strengths are $1.3f'_c$ and $1.17f_y$ for concrete and steel respectively as recommended by the LATBSDC (2005) and PEER/ATC 72-1 (2017) guidelines.

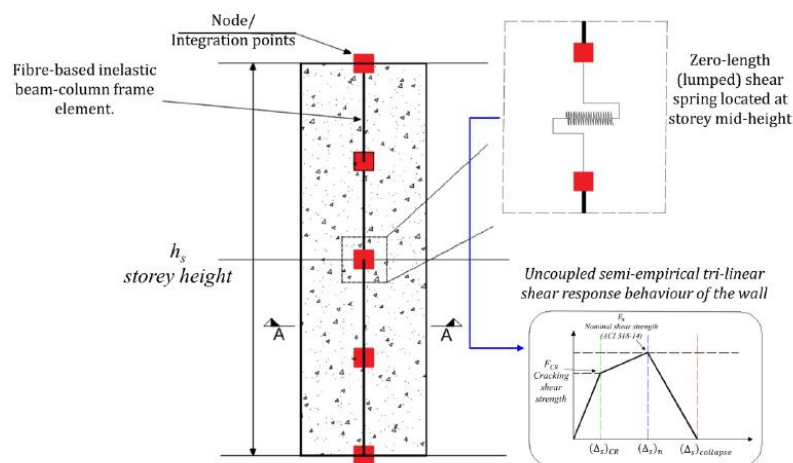
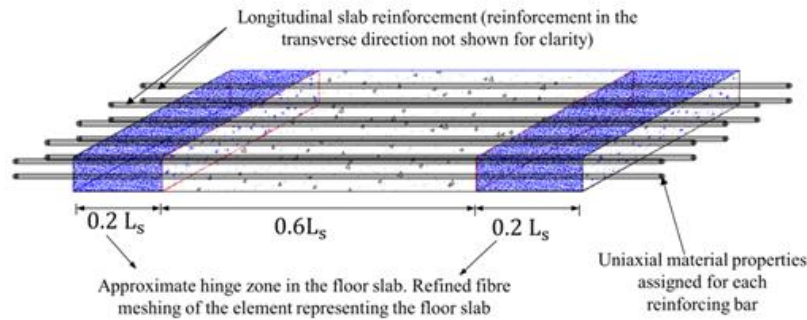
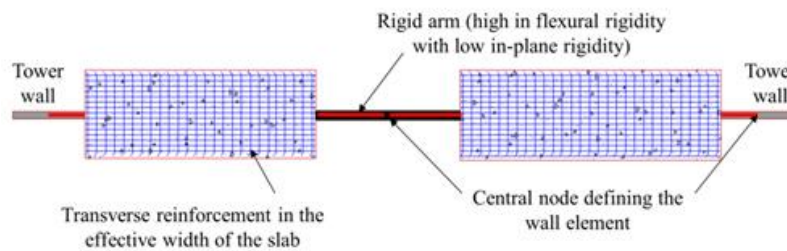


Figure 6 Non-linear modelling of shear walls

The fibre-based inelastic elements were used for modelling the floor slabs and the transfer plate. Only the effective widths (b_{eff}) of the floor slabs have been modelled using the effective width formulae proposed by Grossman (1997). The computed effective width values were found to be approximately 40% of the length of the span in the transverse direction (which is 6.0 m and 8.0 m in the tower and the podium, respectively). The inelastic response behaviour of the floors slabs is characterised by the uni-axial (material) model of the individual fibres. Where concentrations of inelastic demands are anticipated to occur in certain locations along the length of the span, a finer fibre section meshing of the element was adopted (about 20% of the length of the span) as shown in Figure 7a. Conversely, a coarse element discretisation in the rest of the slab (Figure 7a) was used to reduce computational demands. The floor slabs were linked to the walls by means of rigid arms (Figure 7b) as recommended by PEER/ATC 72-1 (2010). Further details on the modelling of load deformation and hysteretic behaviour of the walls, slabs and plates can be found in Yacoubian (2018).



(a) Fibre-meshing of the slabs



(b) Plan-view of the slab showing rigid arm

Figure 7 Modelling of slabs

4 Ground motion inputs

Ground motion inputs were collated to represent a wide range of intensity of Australian earthquakes. The records selected are a combination of: (i) stochastically generated records obtained using the program GENQKE (Lam, 1999) which is capable of producing ground motions that are representative of Australian earthquakes, and (ii) historical records with characteristics that are representative of Australian earthquakes, including shallow earthquakes with reverse fault mechanisms (Brown & Gibson, 2004).

Ground motions on soil were also included in the assessment of RC walls and RC frames buildings. Ground motions on soil were generated by using equivalent linear (Ordonez, 2013) and non-linear site response program DEEPSOIL (Hashash et al., 2016), using generated and historical rock records as input ground motions. It is noted that DEEPSOIL, which is capable of conducting nonlinear analysis, was used for the input records that may have caused the soil strain to exceed the limits for which equivalent linear analyses are valid. The shear wave velocity profiles used to generate the ground motions were obtained from published literature (Roberts et al., 2004; Mc Pherson and Hall, 2007; Kayen et al., 2015).

5 Development of fragility curves

Seismic fragility functions define the building's probability of exceeding a damage limit state as a function of ground motion intensity measure (IM). The fragility function is defined by Equation (1):

$$P[Y > 1|IM] = \phi \frac{\ln(\eta_{Y|IM})}{\sqrt{\beta_{Y|IM}^2 + \beta_C^2 + \beta_M^2}} \quad (1)$$

where, $\eta_{Y|IM}$ is the median critical demand-to-capacity ratio (Y) as a function IM. The demand-to-capacity ratio (Y) is greater than 1.0 when the damage limit based on the performance levels (defined in Section 5.2) has been exceeded. $\beta_{Y|IM}$ is the dispersion (logarithmic standard deviation) of the critical demand-to-capacity ratio as a function of IM. β_C is the capacity uncertainty and β_M is the modelling uncertainty. In this paper, both β_C and β_M were set to zero.

The construction of the fragility functions for the RC shear walls buildings include the variation building type (Figure 1) and the parameters defining the response of the RC walls (Tables 1 and 2), along with the variation in ground motions. The dispersion in the fragility functions for the RC frames buildings and the podium-tower RC buildings was caused by the variation in the ground motions. The median $\eta_{Y|IM}$ and dispersion $\beta_{Y|IM}$ values of the critical demand-to-capacity ratio were obtained following the Multiple Stripe Analysis technique (Baker, 2015) for the RC shear walls and tower-podium RC buildings and the cloud analysis (Jalayer, 2003) for the RC frames buildings.

5.1 Ground motion Intensity Measure (IM)

The development of fragility curves involves conditioning the structural response on the ground motion intensity measure (IM). It is critical that the IM selected shows a strong correlation between the seismic intensity and the structural response to reduce the uncertainty in the seismic assessment. In addition, the IM needs to effectively represent the level of seismic hazard, i.e., it needs to correlate well to earthquake return periods. Traditionally, the IM that has been commonly used for seismic assessment has been peak ground acceleration (PGA). It is the parameter which is typically used to represent hazard on seismic hazard maps, including AS1170.4-2007. However, the seismic hazard factor (Z) in AS 1170.4 is a nominal value obtained from dividing the Peak Ground Velocity (PGV) values (in millimetres per second) by 750 (Wilson and Lam, 2007). This is because PGV is considered to provide a better indication of the level of structural damage since it is related to the energy in the ground motion. In this paper, PGV was used as ground motion IM.

5.2 Definition of Performance levels

There are many different performance levels defined in the literature and codes, each with different acceptance criteria. In this paper, four performance levels were considered: i) slight damage (also often referred to as operational, serviceability or immediate occupancy limit state); ii) moderate damage (also often referred to as damage control or repairable damage limit state); iii) extensive damage (also often referred to as life safety limit state); and iv) complete damage (also often referred to collapse prevention limit state). A summary of the adopted performance levels is provided in Table 6. More details can be found in Amirsardari (2018), Hoult et al. (2018) and Yacoubian (2018).

Table 6 Summary of the adopted performance levels

(a) For RC shear walls buildings (Hoult et al., 2018a)

Performance limit	Primary structure
Slight Damage / Serviceability (S)	Wall reaching a compressive strain of 0.001, or tensile strain of 0.005, whichever occurs first
Moderate Damage/ Damage Control (DC)	Wall reaching a compressive strain of 0.002, or tensile strain of 0.01, whichever occurs first
Extensive Damage/ Life Safety (LS)	Wall reaching ultimate rotational limit, corresponding to a compressive strain of 0.003, or tensile strain of $0.6\varepsilon_{su}$, whichever occurs first
Complete Damage/ Collapse Prevention (CP)	NA

(b) For RC frames buildings (Amirsardari, 2018)

Performance level	Limits		
	Primary structure	Secondary structure	Non-structural limit
Slight Damage / Serviceability (S)	Wall reaching initial yield limit	Frame component reaching nominal yield rotational limit	ISD reaching 0.004
Moderate Damage/ Damage Control (DC)	Wall reaching a compressive strain of 0.002, or tensile strain of 0.015, whichever occurs first	Frame component reaching rotation which is at mid-point between yield and ultimate rotational limits	ISD reaching 0.008
Extensive Damage/ Life Safety (LS)	Wall reaching ultimate rotational limit, corresponding to a compressive strain of 0.004, or tensile strain of $0.6\varepsilon_{su}$, whichever occurs first	Frame component reaches the rotation corresponding to shear failure	ISD reaching 0.015
Complete Damage/ Collapse Prevention (CP)	NA	Frame component reaches the rotation corresponding to 50 % reduction in ultimate lateral strength	ISD reaching 0.002

NA: Not applicable

ISD: Inter-storey drift

(c) For podium-tower RC buildings (Yacoubian, 2018)

Performance level	Limits
Slight Damage / Serviceability	ISD corresponding to the first occurrence of flexural yielding in the RC walls making up the building (in the tower or the podium).
Moderate Damage / Damage Control (DC)	NA
Extensive Damage / Life Safety (LS)	Life safety limit state is defined as the ISD corresponding to: <ol style="list-style-type: none"> 1- Flexural yielding of all the tower walls above the podium interface level (or TFL) 2- Onset of nominal shear force capacity in the tower walls 3- Flexural yielding of the transfer plate (in building models TS-1 and TS-2) <i>Whichever occurs first</i>

Complete Damage / Collapse Prevention (CP)	<p>Collapse prevention limit state is defined as the ISD corresponding to</p> <ol style="list-style-type: none"> 1. Onset of crushing compression strain in the confined core of the RC tower walls $\epsilon_{cu} = -0.003$ 2. 50% loss of lateral strength in the tower walls (Walls 1 & 2) 3. Onset of nominal shear strength capacity of the central wall (ultimate strength) 4. Onset of ultimate tensile strain ($\epsilon_{su} = 0.03$) in the reinforcement. <p><i>Whichever occurs first</i></p>
--	---

ISD: Inter-storey drift

5.3 Fragility curves

Based on the median $\eta_{Y|IM}$ and dispersion $\beta_{Y|IM}$ values, obtained following the Multiple Stripe Analysis technique for the RC shear walls and tower-podium buildings and the cloud analysis for the RC frames buildings, the fragility curve can be derived using Equation (1). The equation calculates the probability of a certain damage limit state being exceeded at a given ground motion intensity (IM) level. The fragility curves for the three types of RC buildings are presented in Figures 8 to 10.

Although different approach in modelling and different parameters have been adopted in the construction of these fragility curves, it can be generally deduced that RC frames buildings are more vulnerable than RC shear walls and podium-tower RC buildings. The height of the buildings was not found to have significant impact on the behaviour of the RC shear walls buildings whilst it has moderate impact on the RC frames buildings (Figures 8 and 9). Podium-tower RC buildings featuring a distinct change in the form of lateral load resisting elements and a transfer structure (TS-1 and TS-2) were found to be more vulnerable than to those with the lateral load resisting elements continuing to the podium levels (SB-1 and SB-2). The higher vulnerability of TS-1 and TS-2 are caused by the adverse effects of the flexibility of the transfer plates on the shear force demand on the tower walls immediately above the transfer plates.

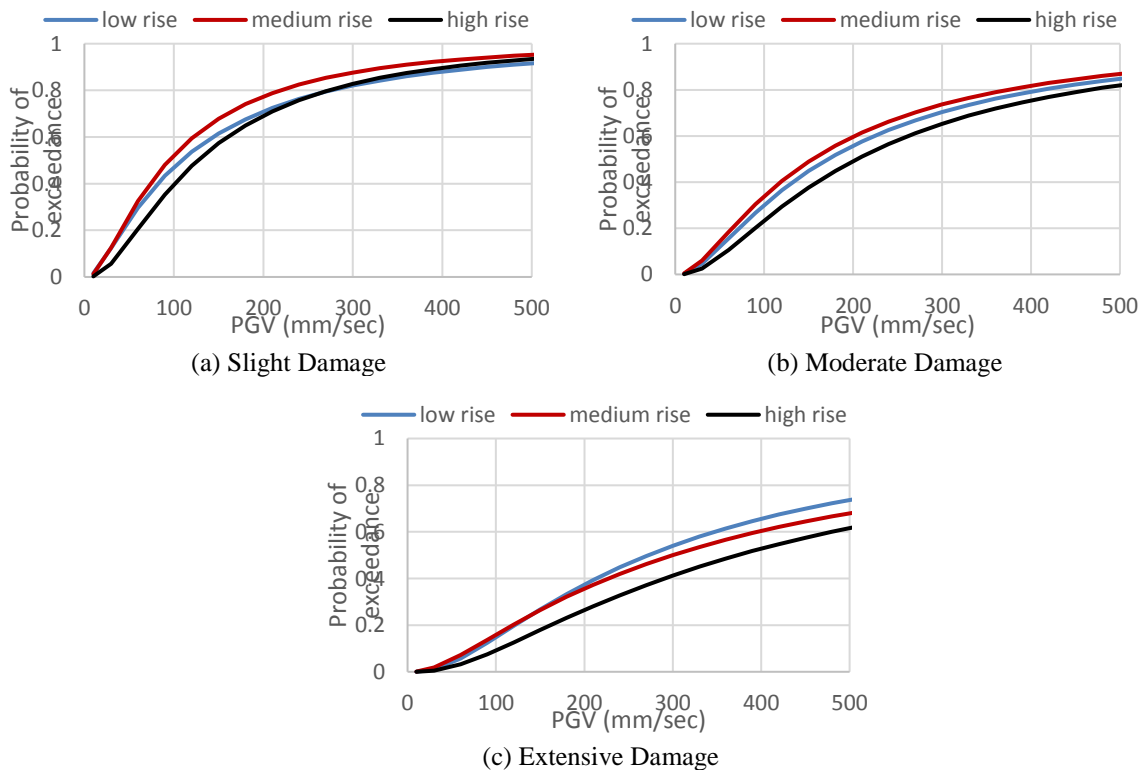


Figure 8 Fragility curve for RC wall buildings

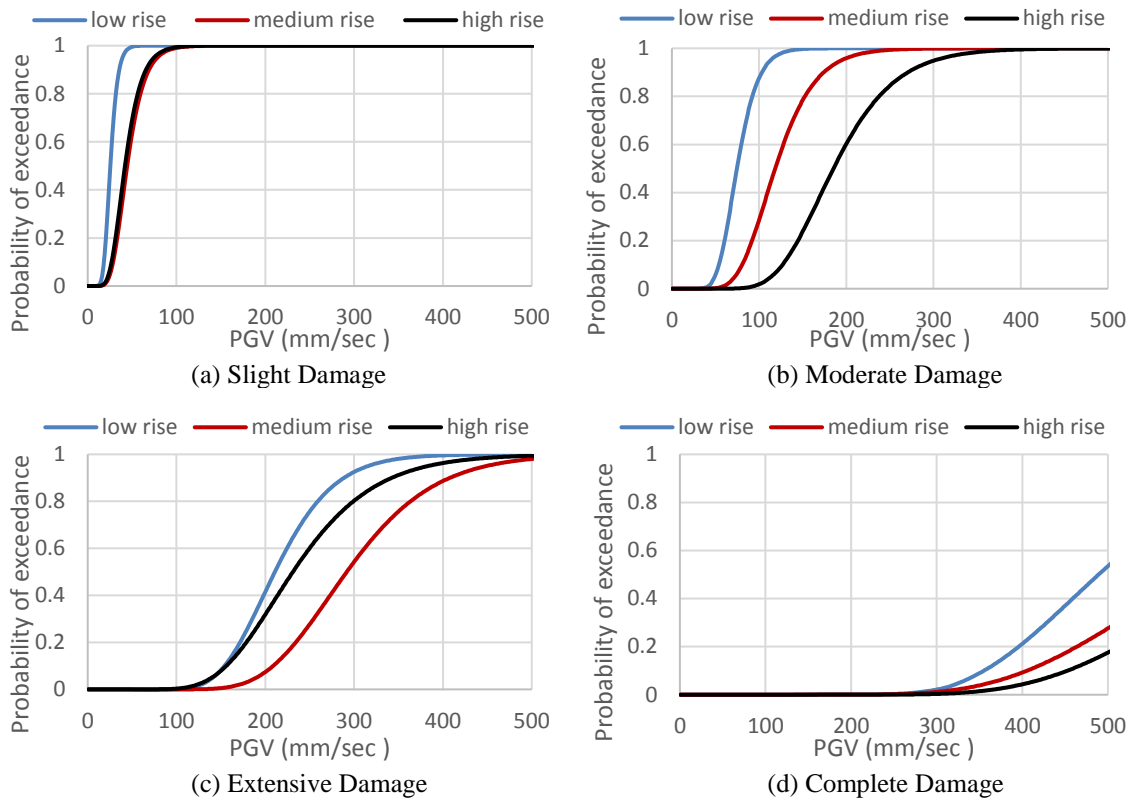


Figure 9 Fragility curves for RC frames building

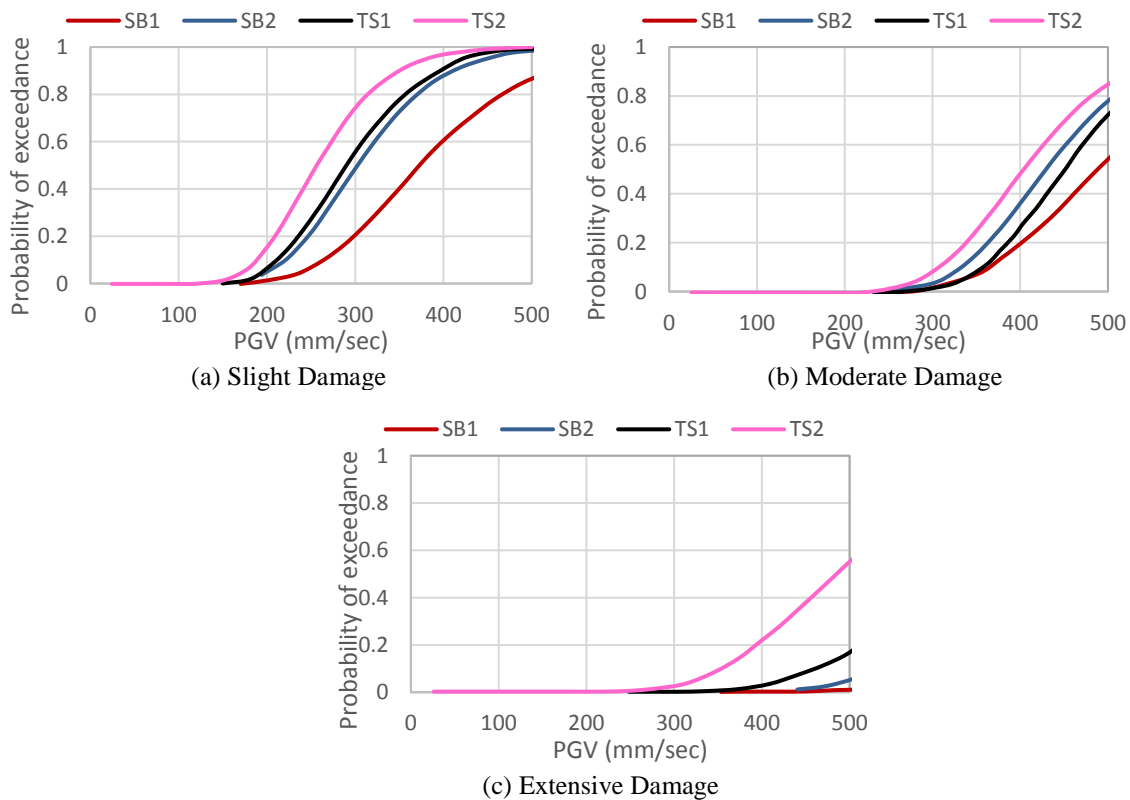


Figure 10 Fragility curves for podium-tower RC buildings

To provide an indication of the performance of the buildings under to a 500 and 2500-year return period event, the PGV values associated with the events were calculated in accordance with AS1170.4-2007. The PGV values are presented in Table 7 for class A to Class D. The

probability of exceedance of a certain damage level associated with PGV values listed in Table 7 are presented in Table 8 for the three types of buildings investigated. It is shown that the slight damage limit is expected to be exceeded under a 500- and 2500-year event for the RC frames and RC shear walls buildings, whilst the probability of the damage level to be exceeded is much lower for the podium-tower RC buildings. Both RC shear walls and RC frames building are shown to have a high probability of the extensive damage limit being exceeded (for the most onerous soil site) under the 2500-year return period event. It is noted that vulnerability of the buildings can be exacerbated by plan asymmetry in the building, which is outside the scope of this paper.

Table 7 PGV values calculated in accordance with AS1170.4-2007 for 500- and 2500-year RP event

Site condition	PGV (cm/s)	
	500 YRP	2500 YRP
Class A	61	110
Class B	76	137
Class C	108	195
Class D	172	309

Table 8 Probability of exceedance under 500- and 2500-year RP event

(a) RC shear walls buildings

Site condition	Limited Damage		Moderate Damage		Extensive Damage	
	500 YRP	2500 YRP	500 YRP	2500 YRP	500 YRP	2500 YRP
Class A	0.30	0.55	0.20	0.40	0.10	0.20
Class B	0.40	0.65	0.25	0.45	0.10	0.25
Class C	0.50	0.75	0.35	0.60	0.20	0.35
Class D	0.80	0.90	0.55	0.75	0.30	0.50

(b) RC frames building

Site condition	Limited Damage		Moderate Damage		Extensive Damage		Complete Damage	
	500 YRP	2500 YRP	500 YRP	2500 YRP	500 YRP	2500 YRP	500 YRP	2500 YRP
Class A	1.0	1.0	0.20	0.95	0.0	0.0	0.0	0.0
Class B	1.0	1.0	0.55	1.0	0.0	0.04	0.0	0.0
Class C	1.0	1.0	0.95	1.0	0.0	0.40	0.0	0.0
Class D	1.0	1.0	1.0	1.0	0.20	0.95	0.0	0.03

(c) Tower-podium building

Site condition	Limited Damage		Moderate Damage		Extensive Damage	
	500 YRP	2500 YRP	500 YRP	2500 YRP	500 YRP	2500 YRP
Class A	0.0	0.0	0.0	0.0	0.0	0.0
Class B	0.0	0.0	0.0	0.0	0.0	0.0
Class C	0.0	0.15	0.0	0.0	0.0	0.0
Class D	0.02	0.75	0.01	0.10	0.0	0.04

6 Concluding Remarks

This paper presents sets of fragility curves for limited ductile reinforced concrete buildings. Fragility curves were presented for limited-ductile reinforced concrete (RC) buildings typical of Australian constructions: i) fragility curves for RC buildings that are primarily supported by limited-ductile RC shear wall (referred to **RC shear walls buildings** in this paper); ii) fragility curves for RC buildings that are supported by limited-ductile RC walls and frames (referred to **RC frames buildings** in this paper); and iii) fragility curves for **podium-tower RC buildings**.

The assessment was conducted by performing nonlinear analyses using the capacity spectrum method and time history analyses of the nonlinear building models. Ground motion records have been selected from a combination of stochastically generated records, historical records with characteristics representative of Australian earthquakes and simulated records on soil conditions. The multi-stripe and cloud analyses have been adopted to compute the fragility functions. The fragility curves for the three types of buildings have been presented in the forms of peak ground velocity as an intensity measure. Although the approach and parameters adopted are different between the three types of buildings, hence the outcomes are not directly comparable, it is shown that RC frames buildings are generally more vulnerable in an earthquake compared to RC shear walls and podium-tower RC buildings. The fragility curves indicate that RC frames and RC shear walls buildings are expected to experience extensive damage under a 2500-year return period earthquake event.

Acknowledgement

The support of the Commonwealth Australia through the Cooperative Research Centre program

References

- American Society of Civil Engineers (ASCE/SEI). (2013). ASCE 41-13: Seismic evaluation and retrofit of existing buildings. Reston, Virginia: American Society of Civil Engineers Standard Reston, Virginia.
- Amirsardari, A. (2018). Seismic assessment of reinforced concrete buildings in Australia including the response of gravity frames. PhD Thesis. Melbourne: The University of Melbourne.
- Baker, J.W. (2015). Efficient analytical fragility function fitting using dynamic structural analysis. *Earthquake Spectra*, 31(1), 579-599.
- Brown, A., & Gibson, G. (2004). A multi-tiered earthquake hazard model for Australia. *Tectonophysics*, 390(1-4), 25-43. doi: 10.1016/j.tecto.2004.03.019
- Edwards, M., Robinson, D., McAneney, K., & Schneider, J. (2004). Vulnerability of residential structures in Australia. Paper presented at the 13th World Conference on Earthquake Engineering, Vancouver.
- Federal Emergency Management Agency (FEMA). (2010). HAZUS-MH MR5 Technical Manual - Earthquake Model. Washington, D.C.: U.S. Department of Homeland Security.
- Federal Emergency Management Agency (FEMA). (2000). FEMA 356, Prestandard and commentary
- Grossman, J.S. (1997). Verification of proposed design methodologies for effective width of slabs in slab-column frames. *ACI Structural Journal*, 94(2), 181-196.
- Hashash, Y.M.A., Musgrove, M.I., Harmon, J.A., Groholski, D R., Phillips, C.A., & Park, D. (2016). DEEPSOIL 6.1. Retrieved from <http://deepsoil.cce.illinois.edu/>
- Hoult, R., Goldsworthy, H., & Lumantarna, E. (2017a). Displacement Capacity of Lightly Reinforced and Unconfined Concrete Structural Walls. Manuscript submitted for publication.
- Hoult, R., Goldsworthy, H., & Lumantarna, E. (2017b). Plastic Hinge Length for Lightly Reinforced Rectangular Concrete Walls. *Journal of Earthquake Engineering*. doi:10.1080/13632469.2017.1286619
- Hoult, R., Goldsworthy, H., & Lumantarna, E. (2018a). Fragility Functions for RC Shear Wall Buildings in Australia. *Earthquake Spectra*.
- Hoult, R. D., Goldsworthy, H., & Lumantarna, E. (2018b). Plastic hinge length for lightly reinforced C-shaped concrete walls. *Journal of Earthquake Engineering*, 1-32.
- Hoult, R., Goldsworthy, H., & Lumantarna, E. (2018c). Plastic hinge length for lightly reinforced rectangular concrete walls. *Journal of Earthquake Engineering*, 22(8), 1447-1478.
- Jalayer, F. (2003). Direct probabilistic seismic analysis: implementing non-linear dynamic assessments. PhD Dissertation, Stanford University.
- Kayen, R.E., Carkin, B.A., Allen, T., Collins, C., McPherson, A., & Minasian, D.L. (2015). Shear-wave velocity and site-amplification factors for 50 Australian sites determined by the spectral

- analysis of surface waves method: U.S. Geological Survey Open-File Report 2014-1264. doi: <http://dx.doi.org/10.3133/ofr20141264>
- Lam, N.T.K. (1999). "GENQKE" User's Guide: Program for generating synthetic earthquake accelerograms based on stochastic simulations of seismological models. Department of Civil and Environmental Engineering, The University of Melbourne, Australia.
- Mander, J.B., Priestley, M.J., & Park, R. (1988). Theoretical stress-strain model for confined concrete. *Journal of structural engineering*, 114(8), 1804-1826.
- McKenna, F., Fenves, G.L., Scott, M.N., & Jeremic, B. (2000). Open System for Earthquake Engineering Simulation (OpenSEES) (Version 2.4.5, 2013): Pacific Earthquake Engineering Research Center, University of California, Berkeley, CA. Retrieved from <http://opensees.berkeley.edu/>
- McPherson, A.A., & Hall, L.S. (2007). Development of the Australian national regolith site classification map (pp. 37): *Geoscience Australia Record 2007/07*.
- Menegotto, M., & Pinto, P.E. (1973). Method of analysis of cyclically loaded R. C. frames including changes in geometry and non-elastic behavior of elements under combined normal force and bending moment. *IABSE Proc.*
- Mergos, P., & Beyer, K. (2014). Modelling shear–flexure interaction in equivalent frame models of slender reinforced concrete walls. *The Structural Design of Tall and Special Buildings*, 23(15), 1171-1189.
- Ordonez, G.A. (2013). SHAKE2000 (Version 9.99.2 - July 2013). Retrieved from <http://www.geomotions.com>
- PEER/ATC72-1. (2010). Modeling and acceptance criteria for seismic design and analysis of tall buildings. Redwood City, CA: Applied Technology Council in cooperation with the Pacific Earthquake Engineering Research Center.
- Popovics, S. (1973). A numerical approach to the complete stress-strain curve of concrete. *Cement and concrete research*, 3(5), 583-599.
- Priestley, M.J.N., Calvi, G.M., & Kowalsky, M.J. (2007). Displacement-based seismic design of structures. Pavia, Italy: IUSS Press.
- Reddiar, M.K.M. (2009). Stress-strain model of unconfined and confined concrete and stress-block parameters. M.S. Dissertation. Texas, U.S.A: Texas A&M University.
- Robinson, D., Fulford, G., & Dhu, T. (2005). EQRM: Geoscience Australia's Earthquake Risk Model. Technical Manual Version 3.0: Record 2005/01: Geoscience Australia: Canberra.
- Roberts, J., Asten, M., Tsang, H. H., Venkatesan, S., & Lam, N. (2004). Shear wave velocity profiling in Melbourne silurian mudstone using the SPAC method. Paper presented at the Australian Earthquake Engineering Society 2004 Conference, Mt Gambier, SA.
- Seckin, M. (1981). Hysteretic Behaviour of Cast-in-Place Exterior Beam-Column-Slab Subassemblies. Ph.D. Thesis. Toronto: University of Toronto.
- SeismoSoft. (2016). A computer program for static and dynamic nonlinear analysis of framed structures. Retrieved from www.seismosoft.com
- Sivaselvan, M.V., & Reinhorn, A.M. (2000). Hysteretic models for deteriorating inelastic structures. *Journal of Engineering Mechanics*, 126(6), 633-640.
- Standards Australia. (1983). Minimum design loads on structures - Wind loads. Sydney, NSW: Standards Association of Australia.
- Standards Australia. (1988). AS 3600-1988: Concrete structures. Sydney, NSW: Standards Association of Australia.
- Standards Australia. (2007). AS 1170.4-2007: Structural design actions, Part 4: Earthquake actions in Australia. Sydney, NSW: SAI Global.
- Standards Australia. (2011). AS 1170.2-2011: Structural design actions, Part 2: Wind Actions. Sydney, NSW: SAI Global.
- Wilson, J., & Lam, N. (2007). AS 1170.4 Supp1-2007 Commentary to Structural Design Actions Part 4: Earthquake Actions in Australia.
- Yacoubian, M. (2018). Podium and transfer structure interference on seismic shear demands of tower walls in buildings. PhD Thesis, Melbourne: The University of Melbourne.